Clinical Biomechanics 37 (2016) 53–59

Contents lists available at ScienceDirect

Clinical Biomechanics

journal homepage: www.elsevier.com/locate/clinbiomech

A biologically-assisted curved muscle model of the lumbar spine: Model structure

Jaejin Hwang [a], Gregory G. Knapik [a], Jonathan S. Dufour [a], Alexander Aurand [a], Thomas M. Best [b], Safdar N. Khan [c], Ehud Mendel [d], William S. Marras [a,*]

[a] Biodynamics Laboratory, Spine Research Institute, The Ohio State University, Department of Integrated Systems Engineering, 1971 Neil Avenue, 210 Baker Systems Engineering, Columbus, OH 43210, USA
[b] Department of Family Medicine, The Ohio State University, Martha Moorehouse Medical Plaza, 2050 Kenny Dr., Columbus, OH 43210, USA
[c] Department of Orthopeadics, College of Medicine, The Ohio State University, Columbus, OH 43210, USA
[d] Department of Neurological Surgery, The Ohio State University, Columbus, OH 43210, USA

ARTICLE INFO

Article history:
Received 8 March 2016
Received in revised form 27 May 2016
Accepted 13 June 2016

Keywords:
Curved muscle
Personalization
Biomechanical model
Model structure
Spine

ABSTRACT

Background: Biomechanical models have been developed to assess the spine tissue loads of individuals. However, most models have assumed trunk muscle lines of action as straight-lines, which might be less reliable during occupational tasks that require complex lumbar motions. The objective of this study was to describe the model structure and underlying logic of a biologically-assisted curved muscle model of the lumbar spine.
Methods: The developed model structure including curved muscle geometry, separation of active and passive muscle forces, and personalization of muscle properties was described. An example of the model procedure including data collection, personalization, and data evaluation was also illustrated.
Findings: Three-dimensional curved muscle geometry was developed based on a predictive model using magnetic resonance imaging and anthropometric measures to personalize the model for each individual. Calibration algorithms were able to reverse-engineer personalized muscle properties to calculate active and passive muscle forces of each individual.
Interpretation: This biologically-assisted curved muscle model will significantly increase the accuracy of spinal tissue load predictions for the entire lumbar spine during complex dynamic occupational tasks. Personalized active and passive muscle force algorithms will help to more robustly investigate person-specific muscle forces and spinal tissue loads.

1. Introduction

Since the 1970s, biomechanical models have been developed to estimate spine tissue loads to quantify the risk of spine disorders for workers in occupational environments. These spine tissue load estimations have usually been compared with the tolerance limit of intervertebral disk endplates, and this relationship has been used to indicate the portion of the population exposed to risk of spine tissue damage in specific work places.

Early on, a static single-equivalent-muscle model was developed to evaluate simple lifting tasks (Chaffin, 1969). However, this model assumed that static postures were representative of lifting movements, focused on trunk extensor muscles exclusively, and assumed those muscles could be represented as a single equivalent trunk muscle group. Only a single component of spine tissue load (compression) was originally calculated, and these models typically assumed that no muscle co-activation occurred during lifting tasks.

Static multiple-muscle models were later developed to account for the various contributions of multiple muscles surrounding the spine during lifting (Schultz and Andersson, 1981). Ten trunk muscles and intra-abdominal pressure were included. This model also considered shear forces as well as compression loads imposed on the spine. Although this approach investigated the effect of multiple muscles on spinal loads, it assumed no antagonistic muscle activity existed during lifting. This assumption was assumed to be appropriate for static lifting exertions but not for dynamic lifting exertions that commonly required greater co-contractions of trunk muscles (Marras et al., 1984). In addition, studies found that ignoring co-contraction of muscles could underestimate spinal loads by up to 70% (Granata and Marras, 1995a,b).

Biologically-assisted models were developed to account for the co-activation of multiple muscles (McGill and Norman, 1986). They

* Corresponding author.
E-mail addresses: hwang.285@osu.edu (J. Hwang), knapik.1@osu.edu (G.G. Knapik), dufour.8@osu.edu (J.S. Dufour), aurand.20@osu.edu (A. Aurand), Tom.Best@osumc.edu (T.M. Best), Safdar.Khan@osumc.edu (S.N. Khan), Ehud.Mendel@osumc.edu (E. Mendel), marras.1@osu.edu (W.S. Marras).

http://dx.doi.org/10.1016/j.clinbiomech.2016.06.002
0268-0033/

measured electromyography (EMG) data as an input to assess muscle coactivity, but were limited to validation during static exertions only. Static stability models were also introduced (Cholewicki and McGill, 1996; Granata and England, 2006), but they were not applicable to dynamic stability behavior.

Dynamic biologically-assisted models were also developed in an effort to account for muscle co-activation during dynamic exertions (Arjmand et al., 2010; Gagnon et al., 2011; Granata and Marras, 1993; Marras and Sommerich, 1991a,b; McGill, 2004; Van Dieen and Kingma, 2005). Some of these advanced models attempted to assess the person-specific spine tissue loads of individual workers during a wide range of dynamic occupational tasks, such as lifting (Arjmand et al., 2011; Marras et al., 2004), pushing/pulling (Knapik and Marras, 2009; Marras et al., 2009), and carrying (Rose et al., 2013; Schibye et al., 2001).

Although advanced models were able to assess biological responses of multiple trunk muscles during dynamic occupational tasks, they assumed the muscle lines of action could be represented as straight-line vectors (Granata and Marras, 1993; Marras and Sommerich, 1991a,b; McGill and Norman, 1986). "Straight-line" muscle models have worked reasonably well in relatively simple tasks that require only a small range of lumbar motions, but this assumption could be less reliable when applied to complex asymmetric lumbar motions that commonly occur in the workplace (Marras et al., 1993). These improper muscle force lines of action assumptions could affect the model's accuracy of predicting three-dimensional spine tissue loads.

Another important limitation of most models is that they have rarely considered the individual variability of muscle properties, such as muscle force-length and force-velocity relationships. Most models assume the same relationship of muscle force-length and force-velocity for all subjects (Christophy et al., 2012; Ghezelbash et al., 2015; Van Dieen and Kingma, 2005), or do not account for these relationships at all (Daggfeldt and Thorstensson, 2003; de Zee et al., 2007). However, previous literatures reported age-related changes of muscle force-length and force-velocity relationships (Thelen, 2003), and variations of optimal sarcomere lengths in humans (Lieber et al., 1994; Walker and Schrodt, 1974). Various slopes and shifts of the muscle force-length and force-velocity relationships directly affect the magnitude and temporal variability of the muscle forces as a function of the changes of muscle length and muscle velocity of individuals. Considering this physiological variability of muscle properties would help to estimate more person-specific muscle forces.

In addition, only a few spine models clearly have distinguished the role of active and passive muscle force in force calculation algorithms (Ghezelbash et al., 2015; Van Dieen and Kingma, 2005). If models only rely on active muscle force components during muscle activities, it is difficult to precisely assess the spinal loads during lumbar flexion relaxation which involves minimal muscle activity but significant passive force (Adams and Hutton, 1986; Ghezelbash et al., 2015; Hajihosseinali et al., 2014).

In order to overcome these issues, a personalized biologically-assisted curved muscle model was developed in the current study. Several curved muscle models have previously been developed for both the cervical spine (Kruidhof and Pandy, 2006; Suderman and Vasavada, 2012; Vasavada et al., 2008) and the thoracic/lumbar spine (Arjmand et al., 2006; Gatton et al., 2001; Stokes et al., 2010; Van Dieen and Kingma, 2005). However, most of these models have not been validated during dynamic exertions and personalization of muscle parameters was seldom considered. In addition, only extensor or only oblique abdominal muscles were generally treated as curved muscles (Arjmand et al., 2006; Stokes et al., 2010). Herein, we developed an approach that overcomes many of the previously discussed limitations in order to better predict spinal tissue loading during complex dynamic occupational tasks that is personalized to each individual. A specific example illustrating the model's fidelity is presented.

2. Model development

2.1. Goals

The goals of this effort were two-fold:

1) Develop accurate three-dimensional curved muscle geometry in the model based on Magnetic Resonance Imaging (MRI)-derived muscle moment-arms and physiological cross-sectional areas (PCSAs) as a function of anthropometric measures.
2) Develop a personalized biologically-assisted muscle force algorithm to account for individual variation of trunk muscle properties including both active and passive muscle gains and muscle force-length and force-velocity relationships.

2.2. Benchmark model structure

The benchmark model structure is consisted of a biologically-assisted straight-line muscle model of the lumbar spine. This model utilized individual anthropometry, kinematics, kinetics, and biological muscle activities to predict the three-dimensional spinal loads during dynamic exertions and has been well validated across different types of occupational tasks (Dufour et al., 2013; Granata and Marras, 1995b, 1993; Knapik and Marras, 2009; Marras and Granata, 1995, 1997a, 1997b; Marras and Sommerich, 1991a, 1991b; Marras et al., 2009, 2004, 2001a; Rose et al., 2013; Theado et al., 2007). The straight-line muscle model represented the trunk muscles as ten force vectors attached between the upper and lower torso. It calculated the spinal loads at multiple lumbar disk levels based on the summation of these multiple muscle force vectors and the inertial contributions of different body segments.

2.3. Curved muscle model structure

Fig. 1 shows the conceptual flow diagram of the biologically-assisted curved muscle model. It illustrates the internal components of the models from model inputs to model outputs, and their interactions. In particular, elements highlighted with a dotted line represent how the curved muscle representation systematically affects multiple components in the model.

With regards to the model inputs, positional data from an optical motion capture system were used to determine the location of the spine and other body segments relative to a force plate. Kinematic data including angle, angular velocity and angular acceleration of the trunk and whole body were used to calculate the trunk muscle length, muscle velocity, and gravitational moments of each body segment. For kinetic data, measured three-dimensional external force and torque from force transducers was used to calculate spinal moments at multiple lumbar levels. The model also utilized EMG data from five pairs (10 muscles) of major power-producing trunk muscles including the latissimus dorsi, erector spinae, rectus abdominis, external oblique, and internal oblique to calculate the biologically-assisted muscle force. Muscle forces were also modulated based on person-specific parameters describing the relative active and passive strength of the muscle, as well as relationships between force and the instantaneous length and velocity of each muscle. Subject anthropometric data including height, body mass, trunk width, and trunk depth measures, and demographic information such as age and gender were required to predict the personalized curved muscle geometry for each individual. An MRI database of muscle moment-arms and PCSAs of the ten trunk muscles at multiple thoracic/lumbar levels was used to develop the precise anatomical curved muscle geometry (Jorgensen et al., 2001; Marras et al., 2001b).

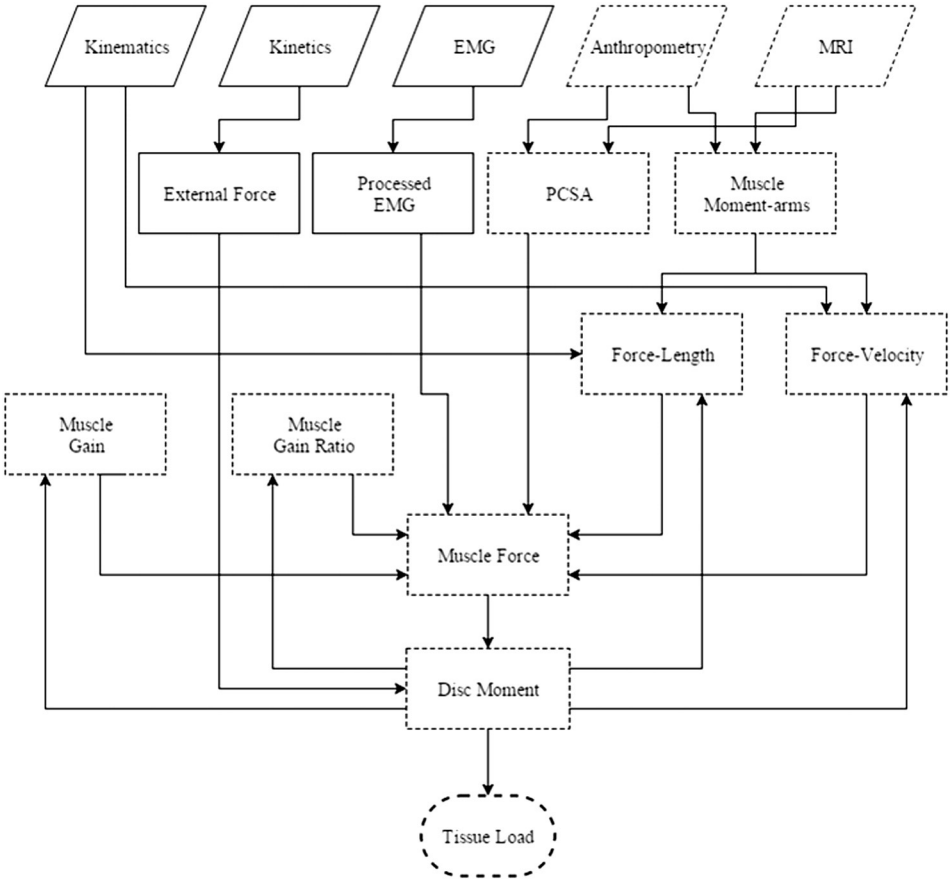

Fig. 1. Biologically-assisted curved muscle model flow diagram. Dotted lines indicate elements of the model whose function was influenced by the use of curved muscle.

2.3.1. Muscle geometry

Muscle moment-arms and PCSAs of trunk muscles at multiple levels through the thoracic/lumbar spine were used to develop three-dimensional curved muscle geometries. Based on MRI-derived muscle moment-arms and PCSAs of 30 subjects (10 males and 20 females) (Jorgensen et al., 2001; Marras et al., 2001b), a polynomial regression model was developed to predict personalized curved muscle geometry as a function of anthropometric measures. The following measures were considered for the regression: vertebral level, sex, age, height, body mass, trunk depth, and trunk width. The polynomial regression coefficients and performances for the sagittal and coronal plane muscle moment-arms (cm) and PCSA (cm^2) can be found elsewhere (Hwang et al., 2016a).

Based on the muscle moment-arm regression model, the curved muscle centroid path (force vectors) was developed for each pair of the latissimus dorsi, erector spinae and rectus abdominis. For the external oblique and internal oblique, the fiber oriented path from previous studies was used (Jorgensen et al., 2001). The fiber orientations of the external oblique and internal oblique were very different from their muscle centroid paths, so fiber oriented path was found to be a more reasonable assumption to estimate muscle force lines of action (Dumas et al., 1991; Jorgensen et al., 2001).

The "via-point" method was used to allow curved muscles to deform with the spinal column during complex dynamic lumbar motions (de Zee et al., 2007; Van Dieen and Kingma, 2005). The "via-points" of each muscle were rigidly linked to the vertebral body of the corresponding lumbar level, and muscle force was transmitted through the "via-points." Seven "via-points" were implemented along each muscle path from T12 to S1.

Multiple PCSAs from the T8 to S1 level of each muscle were also predicted using the polynomial regression model. Fig. 2 shows the visual comparison between the curved muscle and straight-line muscle geometry in a multi-body dynamic simulation environment, ADAMS (MSC Software). Blue lines represent the curved muscle line of action of ten trunk muscles, and multiple points along the muscle path represent the "via-points". The ellipses represent the PCSA of each curved muscle as it changes across the levels of the lumbar spine. The red lines indicate the straight line of action of the ten muscles, and endpoints of muscle paths represent the origin and insertion of muscles.

2.3.2. Biologically-assisted muscle force algorithms

In order to account for the characteristics of curved muscles, a new biologically-assisted muscle force equation was introduced (Eq. (1)).

$$\begin{aligned} F_j(t) &= \text{Active } F_j(t) + \text{Passive } F_j(t) \\ &= \left(GR_j \cdot EMG_j(t) \cdot Area_j \cdot f_{active}\left[L_j(t)\right] \cdot f\left[v_j(t)\right]\right) \\ &\quad + \left(Gain_j \cdot Area_j \cdot f_{passive}\left[L_j(t)\right]\right) \end{aligned} \tag{1}$$

Total muscle force (F) of each muscle (j) was divided into active and passive muscle force. Active mus cle force was derived by the product of (1) Gain Ratio (GR), (2) EMG, (3) PCSA, (4) modulation of active force-length, and (5) force-velocity relationships. Passive muscle force was calculated by the product of (1) Gain, (2) PCSA, and (3) modulation of the passive force-length relationship.

Gain Ratio (GR) describes the Gain (maximum muscle force per unit area) divided by the maximum voluntary contraction (MVC). This property was developed in a previous study to eliminate the need for measuring MVCs and empirically validated during complex free-dynamic

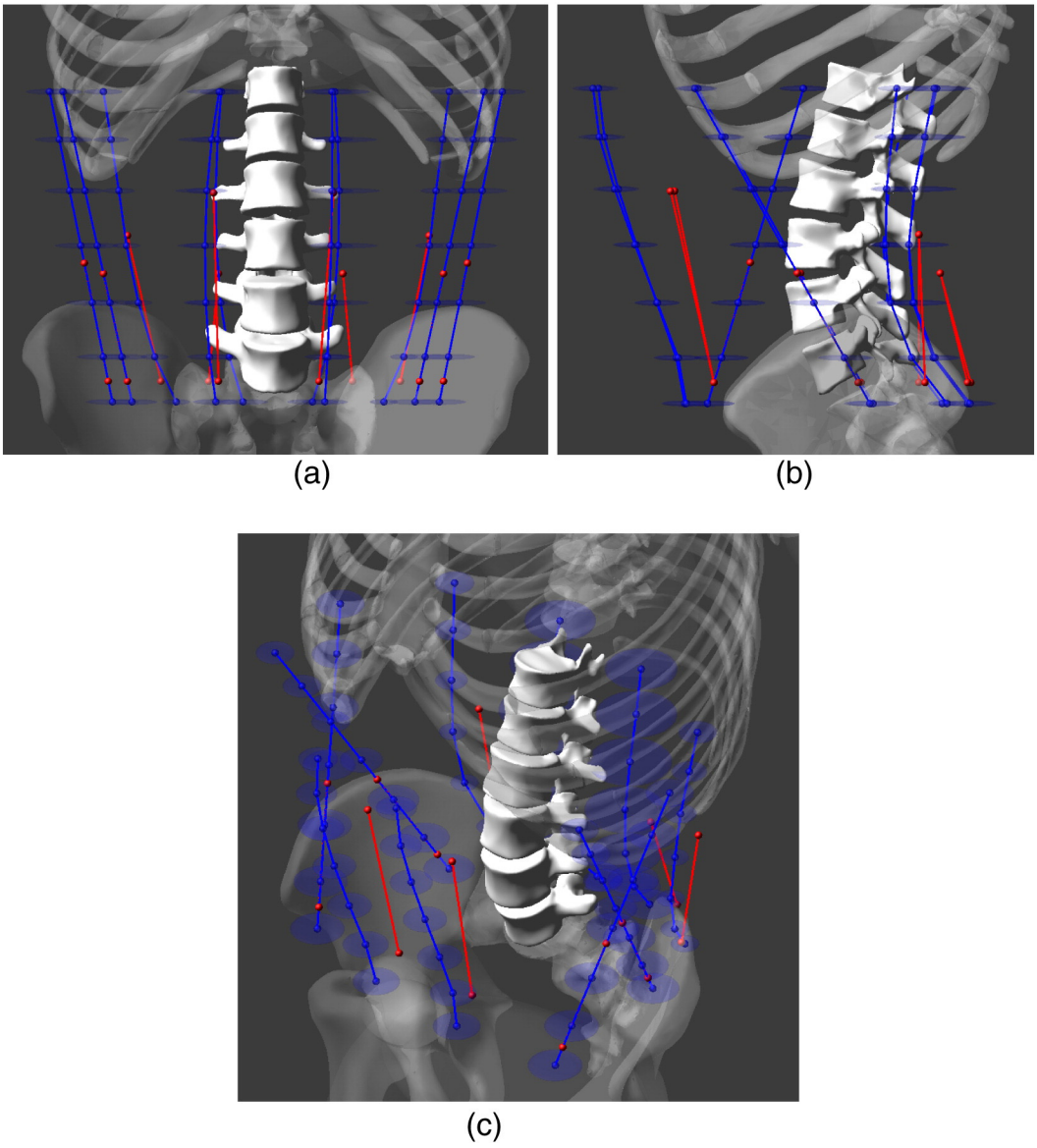

Fig. 2. Three-dimensional graphical representation of curved and straight-line muscle geometry. Note: Blue lines illustrate the curved lines of action of each muscle, and the multiple points along the muscle path indicate the "via-points". Red lines describe the straight lines of action of each muscle, and endpoints of the muscle path indicate the origin and insertion of each muscle. In Panel (c), the different size ellipses of curved muscles represent the variable PCSAs of each muscle through multiple lumbar levels.(For interpretation of the references to color in this figure legend, the reader is referred to the web version of this article.)

conditions (Dufour et al., 2013). EMG represents the muscle activity of each of the 10 trunk muscles. Maximum PCSA for each muscle was considered to estimate the maximum force generation capability.

The active muscle force-length relationship accounts for the capability of each muscle to produce force based on the length of the muscle. The calculation of active muscle force as a function of normalized muscle length was derived from the literature (Cadova et al., 2014; Vilimek, 2007).

The force-velocity relationship was developed to consider the muscle force changes with muscle velocity during eccentric and concentric exertions. The modulations of concentric and eccentric force-velocity relationships were derived from the literature (Close, 1964; Hill, 1938).

Gain values represented the maximum force per unit area of muscles (N/cm^2). The product of Gain and PCSA estimated the maximum muscle force capability of each muscle. The calculation of passive muscle force as a function of normalized muscle length was derived from the literature (McCully and Faulkner, 1983).

2.3.3. Personalized muscle force algorithms

The biologically-assisted model was calibrated to each individual to determine personalized physiological muscle properties. The objective function of the calibration procedure minimized weighted multiplanar root-mean-square error (RMSE) between predicted internal moments and measured external moments of multiple lumbar disk levels from T12/L1 through L5/S1 in the sagittal and lateral physiologic planes. A constrained nonlinear multivariate optimization algorithm was employed to minimize RMSE.

Gain Ratio parameters of all muscles were optimized within a functional boundary (Dufour et al., 2013). Gain values of all muscles were optimized within the physiological boundary from 30 N/cm^2 to 100 N/cm^2 (Close, 1972; McGill and Norman, 1987; Reid et al., 1987; Weis-Fogh and Alexander, 1977). Slope coefficients of force-length and force-velocity relationships were optimized between boundaries found in the literature (Cadova et al., 2014; Close, 1964; Hill, 1938; McCully and Faulkner, 1983; Vilimek, 2007).

2.4. Model procedure

Regarding the data collection procedure, the subjects' anthropometric data were initially measured. The surface electrodes were then placed on the ten trunk muscles to measure muscle activities. An OptiTrack optical motion capture system (NaturalPoint, Corvallis, OR, USA) including 24 Flex 3 infrared cameras was utilized to collect positional and kinematic data. Forty-one reflective motion capture markers were attached to the subjects' body segments and joints to measure kinematics of the whole body via Optitrack's Motive software (http://www.optitrack.com). After setup, subjects were required to stand in an upright posture to measure resting trunk muscle length. The subject was then instructed to perform calibration exertions.

For calibration exertions, subjects stood on two force plates and performed concentric and eccentric lumbar exertions in multiple planes with a 9.07 kg load weight. Subjects were instructed to perform these exertions within comfortable self-selected ranges of motion and speed, and were repeated three times. These exertions encouraged dynamic ranges of muscle length, muscle velocity and muscle activities for each person while exposing them to external moments in all three physiologic planes. This data was used to optimize personalized muscle properties.

Once the optimization was completed, the personalized parameters were set, and used to forward-drive the model throughout the rest of the study. In addition, peak and average spinal load and muscle forces values were calculated. The dynamic biologically-assisted muscle forces of the ten muscles are useful for the investigation of the co-contraction of the agonist and antagonist muscle groups. Model performance measures evaluating the moment matching capability at each of the lumbar disk levels were continuously evaluated as well. This person-specific data was able to compare individual differences in spinal loads and biologically-assisted muscle forces between subjects. Based on estimated spinal loads, it was also able to evaluate the potential risk for injury by comparing spinal loads to spine tolerance limits for the intervertebral disk (Chaffin et al., 2006; Gallagher and Marras, 2012; National Institute for Occupational Safety and Health, 1981).

3. Discussion

The present paper describes the model structure for the developed biologically-assisted curved muscle model of the lumbar spine. The logic behind each component of the model from data collection to evaluation and interpretation is discussed here.

3.1. Model structure logic

Compared to the straight-line muscle model, there were major features introduced in the present approach that bear review. First, a major feature was the development of precise curved muscle geometry through the entire lumbar spine. Second, the muscle force algorithm was modified to consider the contribution of active and passive muscle force, separately. Lastly, the biologically-assisted muscle force algorithms were personalized to account for the muscle length and velocity of curved muscles and individual variances in muscle properties.

3.1.1. Muscle geometry

The goal of the present study was to develop precise curved muscle geometry (using MRI), and allow it to flexibly move along with the spinal column during complex lumbar motions. The muscle centroid path was developed for each bilateral pair of the latissimus dorsi, erector spinae, and rectus abdominis. Muscle forces acting through muscle centroid paths were assumed to be reasonable when muscle fibers are parallel and uniformly distributed (Jensen and Davy, 1975; Rab et al., 1977). Fiber orientations for the latissimus dorsi and rectus abdominis were found consistent with the muscle centroid path (Bogduk et al., 1998; Dumas et al., 1991; Stokes and Gardner-Morse, 1999). The present study used the pair for the erector spinae group that consisted of the transversospinalis and erector spinae based on MRI measurements (Jorgensen et al., 2001; Marras et al., 2001b). When considering the resultant force lines of action of several fascicles, the centroid path approach is considered reasonable for describing the directions of the muscle actions (An et al., 1981). Thus, the left and right erector spinae centroid paths were used to represent the overall resultant lines of action of several fascicles, an approach consistent with other modeling studies (Nussbaum and Chaffin, 1996; Takashima et al., 1979). Fiber-oriented muscle paths were used for the pair of external oblique and internal oblique due to the large fiber orientation relative to the muscle centroid path (Dumas et al., 1991).

In the present study, the single resultant muscle line of action was modeled for each muscle instead of modeling multiple vectors representing several fascicles of each muscle. As a first step, this study focused on the enhancements of curved muscle approach compared to previous straight-line muscle model with a similar set of ten trunk muscles' representations. Thus, employing multiple curved vectors within each muscle was beyond the scope of this study. Nevertheless, for the future study, a development of multiple curved vectors of complex muscles such as oblique and latissimus dorsi would be helpful to accurately model a complex behavior of muscles.

The maximum muscle force (F0) represented the greatest force a muscle could produce at its optimal/resting muscle length (L0), and was highly related to the PCSA. The muscles with larger cross sectional areas (more sarcomeres) generate a larger force, so the largest PCSA of each muscle was selected to estimate the maximum muscle force capability.

3.1.2. Personalized biologically-assisted muscle force algorithm

The goal of this muscle force algorithm was to account for the impact muscle length and velocity have on the force developed in curved muscles. This approach was chosen over using muscle force algorithms that were specifically designed for straight-line muscles because it accounted for the individual variances of several muscle properties. In addition, the new force algorithm was able to personalize and distinguish the contribution of active and passive muscle force.

Straight-line muscle model have utilized empirically-driven muscle force-length and force-velocity relationships for both the flexor and extensor trunk muscle groups (Theado et al., 2007). This method was empirically validated, and worked well during a range of occupational tasks such as lifting (Dufour et al., 2013), pushing/pulling (Knapik and Marras, 2009), and carrying (Rose et al., 2013). However, the empirical force-length and force-velocity relationships were developed based on the specific characteristics of straight-line muscles, and so would not perform well for curved muscles. In addition, these force-length and force-velocity relationships represented the average across a group of subjects, so they could not determine individual differences for each subject.

In order to account for the characteristics of curved muscles, a new muscle force-length relationship was developed in the present study. The active and passive force-length relationships were derived from literature (Cadova et al., 2014; McCully and Faulkner, 1983; Vilimek, 2007). They showed that a high variance of active and passive force-length relationships exists across different muscles (McCully and Faulkner, 1983). In order to account for this variability, physiological boundaries for the active and passive force-length relationships were set (McCully and Faulkner, 1983) and relationships were personalized for each subject tested.

For the muscle force-velocity relationship, similar logic was applied in the present model to account for the characteristics of curved muscles. The equations of the eccentric and concentric force-velocity relationships were derived from previous studies (Close, 1964; Hill, 1938). Not surprisingly, muscle fiber type influenced the force-velocity relationships. Most human muscles are a combination of slow-twitch and fast-twitch fibers. In order to account for the different percentages of

the two major fibers types, physiological boundaries for the eccentric and concentric force-velocity curves were set (Close, 1964; Hill, 1938) and parameters were personalized for each subject during calibration.

3.2. Future improvements

Although the present model considered the individual variation of muscle force-length, muscle force-velocity, and muscle properties, some parameters were not personalized in this model. For instance, personalized bone geometry from MRI and computed tomography (CT) and person-specific material properties of the vertebral bodies, ligaments, and disks were not included in this study. Considering this characteristic would enhance the accuracy of person-specific tissue loads and tolerances. Second, sliding contact force between wrapping muscles and bones were not considered in this study. Considering this mechanical simulation of muscles would increase the accuracy of spine tissue loads during extreme postures (Arjmand et al., 2006).

Even though this study accounted for the muscle tension mechanics via curved muscle paths of abdominal muscles (rectus abdominis and external oblique), the function of intra-abdominal pressure (IAP) was not included in this model. Previous studies suggested that increases in IAP resulted in a reduction in spinal compression (Stokes et al., 2010), and increased lumbar stability (Cholewicki et al., 1999). However, other studies, examining IAP in a large group of subjects concluded there were minimal biomechanical contributions of IAP (Marras and Mirka, 1996). In addition, the validation study for the present model (Hwang et al., 2016b [submitted]) assessed natural lifting exertions that were empirically examined, which generally resulted in minimal activations of abdominal muscles. For these reasons, it was assumed that the impact of the IAP on spinal loading would not be substantial within the current scope of this study. Nonetheless, accurate representation of IAP using curved muscles might be considered in future studies.

4. Conclusions

The model structure of a novel biologically-assisted curved muscle model was described in this study. This model introduced several new features including precise curved muscle geometry, separation of active and passive muscle force, and personalized muscle force-length and force-velocity relationships. This model allows for the reliable assessment of person-specific spine tissue loading along the entire lumbar spine during complex dynamic exertions. Lastly, this model has been experimentally validated during complex dynamic exertions. The model fidelity was assessed using measures such as spinal moment-matching capability and spine tissue load estimations as a function of complex physical lifting conditions. A companion article (Hwang et al., 2016b [submitted]) describes the detailed information of the model validation.

Conflict of interest statement

None.

Acknowledgments

None.

References

Adams, M.A., Hutton, W.C., 1986. Has the lumbar spine a margin of safety in forward bending? Clin. Biomech. 1, 3–6.
An, K.N., Hui, F.C., Morrey, B.F., Linscheid, R.L., Chao, E.Y., 1981. Muscles across the elbow joint: a biomechanical analysis. J. Biomech. 14, 659–669.
Arjmand, N., Gagnon, D., Plamondon, A., Shirazi-Adl, A., Larivière, C., 2010. A comparative study of two trunk biomechanical models under symmetric and asymmetric loadings. J. Biomech. 43, 485–491.
Arjmand, N., Plamondon, A., Shirazi-Adl, A., Larivière, C., Parnianpour, M., 2011. Predictive equations to estimate spinal loads in symmetric lifting tasks. J. Biomech. 44, 84–91.
Arjmand, N., Shirazi-Adl, A., Bazrgari, B., 2006. Wrapping of trunk thoracic extensor muscles influences muscle forces and spinal loads in lifting tasks. Clin. Biomech. 21, 668–675.
Bogduk, N., Johnson, G., Spalding, D., 1998. The morphology and biomechanics of latissimus dorsi. Clin. Biomech. 13, 377–385.
Cadova, M., Vilimek, M., Daniel, M., 2014. A comparative study of muscle force estimates using Huxley's and Hill's muscle model. Comput. Methods Biomech. Biomed. Engin. 17, 311–317.
Chaffin, D.B., 1969. A computerized biomechanical model—development of and use in studying gross body actions. J. Biomech. 2, 429–441.
Chaffin, D.B., Andersson, G., Martin, B.J., 2006. Occupational Biomechanics. fourth ed. (Wiley New York).
Cholewicki, J., Juluru, K., McGill, S., 1999. Intra-abdominal pressure mechanism for stabilizing the lumbar spine. J. Biomech. 32, 13–17.
Cholewicki, J., McGill, S.M., 1996. Mechanical stability of the in vivo lumbar spine: implications for injury and chronic low back pain. Clin. Biomech. 11, 1–15.
Christophy, M., Senan, N.A.F., Lotz, J.C., O'Reilly, O.M., 2012. A musculoskeletal model for the lumbar spine. Biomech. Model. Mechanobiol. 11, 19–34.
Close, R., 1964. Dynamic properties of fast and slow skeletal muscles of the rat during development. J. Physiol. 173, 74–95.
Close, R.I., 1972. Dynamic properties of mammalian skeletal muscles. Physiol. Rev. 52, 129–197.
Daggfeldt, K., Thorstensson, A., 2003. The mechanics of back-extensor torque production about the lumbar spine. J. Biomech. 36, 815–825.
de Zee, M., Hansen, L., Wong, C., Rasmussen, J., Simonsen, E.B., 2007. A generic detailed rigid-body lumbar spine model. J. Biomech. 40, 1219–1227.
Dufour, J.S., Marras, W.S., Knapik, G.G., 2013. An EMG-assisted model calibration technique that does not require MVCs. J. Electromyogr. Kinesiol. 23, 608–613.
Dumas, G.A., Poulin, M.J., Roy, B., Gagnon, M., Jovanovic, M., 1991. Orientation and moment arms of some trunk muscles. Spine 16, 293–303.
Gagnon, D., Arjmand, N., Plamondon, A., Shirazi-Adl, A., Larivière, C., 2011. An improved multi-joint EMG-assisted optimization approach to estimate joint and muscle forces in a musculoskeletal model of the lumbar spine. J. Biomech. 44, 1521–1529.
Gallagher, S., Marras, W.S., 2012. Tolerance of the lumbar spine to shear: a review and recommended exposure limits. Clin. Biomech. 27, 973–978.
Gatton, M., Pearcy, M., Pettet, G., 2001. Modelling the line of action for the oblique abdominal muscles using an elliptical torso model. J. Biomech. 34, 1203–1207.
Ghezelbash, F., Arjmand, N., Shirazi-Adl, A., 2015. Effect of intervertebral translational flexibilities on estimations of trunk muscle forces, kinematics, loads, and stability. Comput. Methods Biomech. Biomed. Engin. 18, 1760–1767.
Granata, K.P., England, S.A., 2006. Stability of dynamic trunk movement. Spine 31, E271–E276.
Granata, K.P., Marras, W.S., 1995a. The influence of trunk muscle coactivity on dynamic spinal loads. Spine 20, 913–919.
Granata, K.P., Marras, W.S., 1995b. An EMG-assisted model of trunk loading during free-dynamic lifting. J. Biomech. 28, 1309–1317.
Granata, K.P., Marras, W.S., 1993. An EMG-assisted model of loads on the lumbar spine during asymmetric trunk extensions. J. Biomech. 26, 1429–1438.
Hajihosseinali, M., Arjmand, N., Shirazi-Adl, A., Farahmand, F., Ghiasi, M.S., 2014. A novel stability and kinematics-driven trunk biomechanical model to estimate muscle and spinal forces. Med. Eng. Phys. 36, 1296–1304.
Hill, A.V., 1938. The heat of shortening and the dynamic constants of muscle. Proc. R. Soc. Lond. B Biol. Sci. 126, 136–195.
Hwang, J., Dufour, J.S., Knapik, G.G., Best, T.M., Khan, S.N., Mendel, E., Marras, W.S., 2016a. Prediction of Magnetic Resonance Imaging-Derived Trunk Muscle Geometry with Application to Spine Biomechanical Modeling. Clin, Biomech. http://dx.doi.org/10.1016/j.clinbiomech.2016.06.001.
Hwang, J., Knapik, G.G., Dufour, J.S., Best, T.M., Khan, S.N., Mendel, E., Marras, W.S., 2016b. A Biologically-assisted Curved Muscle Model of the Lumbar Spine: Model Validation. Clin, Biomech (In review).
Jensen, R.H., Davy, D.T., 1975. An investigation of muscle lines of action about the hip: a centroid line approach vs the straight line approach. J. Biomech. 8, 103–110.
Jorgensen, M.J., Marras, W.S., Granata, K.P., Wiand, J.W., 2001. MRI-derived moment-arms of the female and male spine loading muscles. Clin. Biomech. 16, 182–193.
Knapik, G.G., Marras, W.S., 2009. Spine loading at different lumbar levels during pushing and pulling. Ergonomics 52, 60–70.
Kruidhof, J., Pandy, M.G., 2006. Effect of muscle wrapping on model estimates of neck muscle strength. Comput. Methods Biomech. Biomed. Engin. 9, 343–352.
Lieber, R.L., Loren, G.J., Fridén, J., 1994. In vivo measurement of human wrist extensor muscle sarcomere length changes. J. Neurophysiology 71, 874–881.
Marras, W.S., Davis, K.G., Ferguson, S.A., Lucas, B.R., Gupta, P., 2001a. Spine loading characteristics of patients with low back pain compared with asymptomatic individuals. Spine 26, 2566–2574.
Marras, W.S., Ferguson, S.A., Burr, D., Davis, K.G., Gupta, P., 2004. Spine loading in patients with low back pain during asymmetric lifting exertions. Spine J. Off. J. North Am. Spine Soc. 4, 64–75.
Marras, W.S., Granata, K.P., 1997a. Spine loading during trunk lateral bending motions. J. Biomech. 30, 697–703.
Marras, W.S., Granata, K.P., 1997b. The development of an EMG-assisted model to assess spine loading during whole-body free-dynamic lifting. J. Electromyogr. Kinesiol. Off. J. Int. Soc. Electrophysiol. Kinesiol. 7, 259–268.
Marras, W.S., Granata, K.P., 1995. A biomechanical assessment and model of axial twisting in the thoracolumbar spine. Spine 20, 1440–1451.

Marras, W.S., Jorgensen, M.J., Granata, K.P., Wiand, B., 2001b. Female and male trunk geometry: size and prediction of the spine loading trunk muscles derived from MRI. Clin. Biomech. 16, 38–46.
Marras, W.S., King, A.I., Joynt, R.L., 1984. Measurement of loads on the lumbar spine under isometric and isokinetic conditions. Spine 9, 176–187.
Marras, W.S., Knapik, G.G., Ferguson, S., 2009. Loading along the lumbar spine as influence by speed, control, load magnitude, and handle height during pushing. Clin. Biomech. 24, 155–163.
Marras, W.S., Lavender, S.A., Leurgans, S.E., Rajulu, S.L., Allread, W.G., Fathallah, F.A., Ferguson, S.A., 1993. The role of dynamic three-dimensional trunk motion in occupationally-related low back disorders: the effects of workplace factors, trunk position, and trunk motion characteristics on risk of injury. Spine 18, 617–628.
Marras, W.S., Mirka, G.A., 1996. Intra-abdominal pressure during trunk extension motions. Clin. Biomech. 11, 267–274.
Marras, W.S., Sommerich, C.M., 1991a. A three-dimensional motion model of loads on the lumbar spine: I. Model structure. Hum. Factors J. Hum. Factors Ergon. Soc. 33, 123–137.
Marras, W.S., Sommerich, C.M., 1991b. A three-dimensional motion model of loads on the lumbar spine: II. Model validation. Hum. Factors 33, 139–149.
McCully, K.K., Faulkner, J.A., 1983. Length-tension relationship of mammalian diaphragm muscles. J. Appl. Physiol. 54, 1681–1686.
McGill, S.M., 2004. Linking latest knowledge of injury mechanisms and spine function to the prevention of low back disorders. J. Electromyogr. Kinesiol. 14, 43–47 (State of the art research perspectives on muscoskeletal disorder causation and control).
McGill, S.M., Norman, R.W., 1987. Effects of an anatomically detailed erector spinae model on L4L5 disc compression and shear. J. Biomech. 20, 591–600.
McGill, S.M., Norman, R.W., 1986. Partitioning of the L4-L5 dynamic moment into disc, ligamentous, and muscular components during lifting. Spine 11, 666–678.
National Institute for Occupational Safety and Health, 1981. Work practices guide for manual lifting. US Dept. of Health and Human Services, Public Health Service, Centers for Disease Control, National Institute for Occupational Safety and Health, Division of Biomedical and Behavioral Science.
Nussbaum, M., Chaffin, D., 1996. Development and evaluation of a scalable and deformable geometric model of the human torso. Clin. Biomech. 11, 25–34.
Rab, G.T., Chao, E.Y., Stauffer, R.N., 1977. Muscle force analysis of the lumbar spine. Orthop. Clin. North Am. 8, 193–199.
Reid, J.G., Costigan, P.A., Comrie, W., 1987. Prediction of trunk muscle areas and moment arms by use of anthropometric measures. Spine 12, 273–275.
Rose, J.D., Mendel, E., Marras, W.S., 2013. Carrying and spine loading. Ergonomics 56, 1722–1732.
Schibye, B., Søgaard, K., Martinsen, D., Klausen, K., 2001. Mechanical load on the low back and shoulders during pushing and pulling of two-wheeled waste containers compared with lifting and carrying of bags and bins. Clin. Biomech. 16, 549–559.
Schultz, A.B., Andersson, G.B., 1981. Analysis of loads on the lumbar spine. Spine 6, 76–82.
Stokes, I.A.F., Gardner-Morse, M.G., Henry, S.M., 2010. Intra-abdominal pressure and abdominal wall muscular function: spinal unloading mechanism. Clin. Biomech. 25, 859–866.
Stokes, I.A., Gardner-Morse, M., 1999. Quantitative anatomy of the lumbar musculature. J. Biomech. 32, 311–316.
Suderman, B.L., Vasavada, A.N., 2012. Moving muscle points provide accurate curved muscle paths in a model of the cervical spine. J. Biomech. 45, 400–404.
Takashima, S.T., Singh, S.P., Haderspeck, K.A., Schultz, A.B., 1979. A model for semiquantitative studies of muscle actions. J. Biomech. 12, 929–939.
Theado, E.W., Knapik, G.G., Marras, W.S., 2007. Modification of an EMG-assisted biomechanical model for pushing and pulling. Int. J. Ind. Ergon. 37, 825–831 (Musculoskeletal Load of Push–Pull Tasks).
Thelen, D.G., 2003. Adjustment of muscle mechanics model parameters to simulate dynamic contractions in older adults. J. Biomech. Eng. 125, 70–77.
Van Dieen, J.H., Kingma, I., 2005. Effects of antagonistic co-contraction on differences between electromyography based and optimization based estimates of spinal forces. Ergonomics 48, 411–426.
Vasavada, A.N., Lasher, R.A., Meyer, T.E., Lin, D.C., 2008. Defining and evaluating wrapping surfaces for MRI-derived spinal muscle paths. J. Biomech. 41, 1450–1457.
Vilimek, M., 2007. Musculotendon forces derived by different muscle models. Acta Bioeng. Biomech. Wroc. Univ. Technol. 9, 41–47.
Walker, S.M., Schrodt, G., 1974. I segment lengths and thin filament periods in skeletal muscle fibers of the rhesus monkey and the human. Anat. Rec. 178, 63–81.
Weis-Fogh, T., Alexander, R.M., 1977. The sustained power output from striated muscle. Scale Eff. Anim. Locomot. 511–525.